Combustion and Flame 258 (2023) 113078

Contents lists available at ScienceDirect

Combustion and Flame

journal homepage: www.elsevier.com/locate/combustflame

Numerical investigation of the hybrid pulse–DC plasma assisted ignition and NO_x emission of $NH_3/N_2/O_2$ mixture

Yifan Qiu[a], Yifei Zhu[b,*], Yun Wu[c,d], Ningqiu Zhao[c], Zhenyang Li[c], Mai Hao[b], Boya Zhang[b], Di Pan[e]

[a] School of Energy and Power Engineering, Xi'an Jiaotong University, Xi'an, 710049, China
[b] School of Electrical Engineering, Xi'an Jiaotong University, Xi'an, 710049, China
[c] Institute of Aero-engine, School of Mechanical Engineering, Xi'an Jiaotong University, Xi'an, 710049, China
[d] National Key Lab of Aerospace Power System and Plasma Technology, Airforce Engineering University, Xi'an, 710038, China
[e] Deparment of Science, Airforce Engineering University, Xi'an, 710038, China

ARTICLE INFO

Article history:
Received 20 April 2023
Revised 12 September 2023
Accepted 13 September 2023

Keywords:
Non-equilibrium plasma
Ammonia combustion
Ignition
Chemistry modeling
Hybrid nanosecond and DC discharge

ABSTRACT

The ignition delay and NO emission characteristics of the $NH_3/N_2/O_2$ mixture under the influence of pulse–DC hybrid plasma discharges have been studied. The plasma and combustion chemistry mechanisms for $NH_3/N_2/O_2$ mixture are reviewed, an improved kinetics mechanism is proposed with a well validated electron scattering cross section data. An improved coupled plasma and combustion chemistry code allowing sensitivity/pathway analysis is developed. The role of key species on the ignition delay time and the effects of low E/N discharge over long periods of time (DC stage) on NO_x emission are studied. The results show that, NO emission will be strongly enhanced due to the increased HNO, NH and N density in NH_3 containing mixtures in the DC stage, NO density increases with the E/N value in DC stage due to the reduction of NH and NH_2 species. The role of $O_2(a^1\Delta_g)$ in promoting ignition was studied using different rate constant of $O_2(a^1\Delta_g) + NO \rightarrow O_2 + NO$: $O_2(a^1\Delta_g)$ mainly reacts with H_2 and H to produce radicals such as O, H and OH instead of quenched by NO. The vibrationally excited $NH_3(v2)$ molecule plays the dominating role in heat release through V–T relaxation with NH_3.

1. Introduction

Combustion has been the main source of energy for industrial activities worldwide. However, the use of conventional fossil fuels can produce large amounts of CO_2. With the global warming becoming more and more serious, finding energy sources with high energy density and low emissions is becoming increasingly important. As an important hydrogen storage substance, ammonia is considered a strong candidate as a substitute for fossil fuels.

Ammonia is now widely used as a raw material in various industrial products and as a refrigerant in large industrial coolers. The ammonia-related industry has a history of over 100 years and has mature technology in its production, storage, transportation and utilization [1,2]. On the one hand, the liquid ammonia has a higher volume energy density than liquid hydrogen and batteries, which is one of its attractive qualities that makes it attractive for energy storage and transportation [3]. On the other hand, the storage requirements for ammonia are similar to those for propane: it exists in liquid form when pressurized to 9.90 atm at room temperature (25 °C) or −33.4 °C at atmospheric pressure [2]. All these advantages indicate that ammonia is a suitable candidate for replacing fossil fuels with lower investment and higher feasibility. However, there are a some issues that need to be addressed before the widespread use of ammonia as fuel, such as its narrow ignition limit and high NO emission [2,4].

Over the past few decades, plasma has proven to be a promising technology to enhance combustion, reduce emissions, and improve fuel reforming [4–7]. As the fourth state of matter, plasma can introduce new excited particles and large numbers of ions into combustion system to generate new reaction paths. For example, the high-energy electrons/ions can collide with oxygen molecules to generate oxygen atoms, thus generating dynamic effects. Moreover, plasma can also produce thermal effects by increasing the gas temperature through the quenching of excited particles [8,9]. These effects described above can significantly improve the efficiency of fuel oxidation. Therefore, the plasma can offer new possibilities for combustion control and emission control.

---

* Corresponding author.
E-mail address: yifei.zhu.plasma@gmail.com (Y. Zhu).

https://doi.org/10.1016/j.combustflame.2023.113078
0010-2180/

Lefkowitz et al. [10] first investigated the combustion of $NH_3/O_2/He$ mixtures under nanosecond pulse discharge using a zero-dimensional solver coupled ZDPlasKin and CHEMKIN. It was found that at atmospheric pressure and an initial temperature of 1500 K, a small number of pulses applied at a moderate frequency advanced the ignition delay time by 40–60% compared to an instantaneous thermal energy deposition with the same total energy. The radicals created and sustained in the fast-pulsed discharge support reactions at all temperatures, which shows that it is possible to ignite ammonia using non-thermal plasma.

Subsequently, in terms of experiments, Zhu et al. [11] studied the effect of gliding arc plasma on ammonia combustion by adopting optical emission spectroscopy (OES) combined with filter imaging method. They found that gliding arc plasma could generate a large number of oxygen atoms and promote the dissociation of ammonia to generate H atoms, thus promoting the combustion of NH_3. Lin et al. [12] combined a gliding arc plasma reactor with a cyclone burner to investigate the effects of gas discharge medium, equivalent ratio and gas flow rate on flame stability, flame velocity and NO emission. The experimental results show that the air gliding arc plasma and ammonia gas sprayed by the cyclone ring of the burner can promote the ammonia combustion performance significantly, including combustion limitation and NO emission.

Recently, Shahsavari et al. [13] investigated the effect of nanosecond pulse discharge plasma on the ignition delay time and flame characteristics of ammonia over a wide range of reduced electric fields, pulse energy density, mixture temperature and composition by coupling the ZDPlasKin and Cantera codes. The results show that the nanosecond discharge produces more plasma species during the pulse and the flame thickness is not monotonically dependent on the pulse energy density. Taneja et al. [14] assembled an NH_3/air mechanism and discussed the effects of the reduced electric fields (E/N), equivalence ratio, pressure, pulse frequency and energy density on $NH_3/N_2/O_2$ ignition delay time and NO/NO_2 emissions. Mao and Zhong et al. [15–17] studied the effect of non-equilibrium excitation on the ignition enhancement of NH_3/air mixtures in plasma discharges. O and $O(^1D)$ were found to be more effective at enhancing ignition than electron collision reactions dissociating the fuel.

It has to be noted that, the chemical reactions involved in the excited state particles can be further perfected in the mechanisms used in the existing simulation studies. For example, the vibrationally excited states included in the existing mechanism are mainly $N_2(v)$ and $O_2(v)$, the relevant reactions containing $NH_3(v)$ are not very sufficient. In addition the reactions involving excited states are mainly common species such as H_2, H_2O, H etc., with few reactions between vibrationally excited state particles and NH_3, NH_2 and NH etc. Therefore, it is necessary to include more excited–particle–related reactions to allow for a fuller consideration of the way in which the plasma contributes to the combustion. The accuracy of the cross sections has a significant impact on the electron energy distribution function, while the cross sections for NH_3 are not validated firmly by experimental data, therefore the accuracy of the cross sections currently used is not clear. Moreover, from the works of Mao [18,19], it is clear that nanosecond (NS) hybrid DC discharge can promote the generation of electronically excited particle $O_2(a^1\Delta_g)$, a long–lived particle, which is very effective in promoting ignition and it is known to us that difficulty in ignition is an important limiting factor in the use of ammonia. However, as the existing studies are all NS discharge, where the $O_2(a^1\Delta_g)$ density is low, the contribution of this particle to ignition in the $NH_3/O_2/N_2$ mixture and its mechanism are not clear. NO_x is an important air pollutant and its emission is a essential control for NH_3 combustion due to the large number of N atoms it contains. Similarly, with the addition of DC discharge, does the addition of large amounts of $O_2(a^1\Delta_g)$ have an effect on NO_x production. All of the above require further research.

Therefore, in this paper we investigate the ignition delay time and NO_x production of $NH_3/N_2/O_2$ under a hybrid repetitive nanosecond pulse and DC discharge. In Section 2, we present the numerical model, the kinetics schemes and their validations. The definition of initial conditions and the reduced electric fields are given in Section 2.4. The temporal evolution of gas temperature under the influence of nanosecond pulse hybrid DC discharge was calculated, and its deep influence mechanism was obtained through path analysis and sensitivity analysis in Section 3.1. In Section 3.2 the effect on NO generation was studied, and the change of NO generation path and the consumption path under the influence of DC discharge were analyzed. Finally, conclusions are provided in Section 4.

2. Models and chemistry mechanisms

2.1. The coupled combustion and plasma chemistry model

A hybrid plasma-combustion code has been developed and used in the community of plasma assisted ignition and combustion [20]. The code combined the capability of ignition prediction (based on the F77 SENKIN code [21]) and plasma chemistry prediction (based on the famous ZDPlaskin code [22]) and has been successfully used in analyzing the coupling effects between plasma and combustion in various mixtures (e.g. methane, hydrogen). In this work, we rewrite a coupled plasma and combustion chemistry solver (named CPCC in the following text) by combing the ZDPlaskin code with a home–made simple combustion code with F90 format, adding sensitivity and path flux analysis module to make the code compatible with widely used post–processing software (e.g. Pumpkin [23] and QtPlaskin [24]). The calculation process can be summarized as the follows.

We divide each time step into two processes: plasma chemistry process and combustion chemistry process. Plasma chemistry process is solved with the help of the ZDPlaskin, a code coupling BOLSIG+ [25] module to solve dynamically the electron energy distribution function (EEDF) and the density variations of electrons, excited species and ions in a plasma discharge system. The EEDF is the key to the accuracy of plasma chemistry and the reaction rates associated with electron collisions, the accuracy is linked closely with the cross sections of electron collision reactions.

The time evolution of plasma species density is obtained in ZDPlaskin by solving following set of coupled rate equations:

$$\frac{d[N_i]}{dt} = \sum_{j=1}^{j_{\max}} S_{ij}(t) \quad i = 1 \ldots i_{\max} \tag{1}$$

where $[N_i]$, S_{ij}, $i_{\max}$ and $j_{\max}$ represent the concentration of the ith particle, contribution of different reactions to the change in concentration of this particle, number of particles and reactions in the model respectively. The VODE solver [26] was used to solve the ordinary differential equations of particle concentration as input for the combustion chemistry solver.

The gas heating of the discharge is calculated using the method proposed in Ref. [27]: the heating power P_{ext} is classified as three channels: the translational degree of freedom of electrons P_{elec}, the translational degree of freedom of the gas P_{gas} the internal degree of freedom of the gas P_{chem}:

$$P_{ext} = P_{gas} + P_{elec} + P_{chem} \tag{2}$$

$$P_{ext} = eN_e \upsilon_e E \tag{3}$$

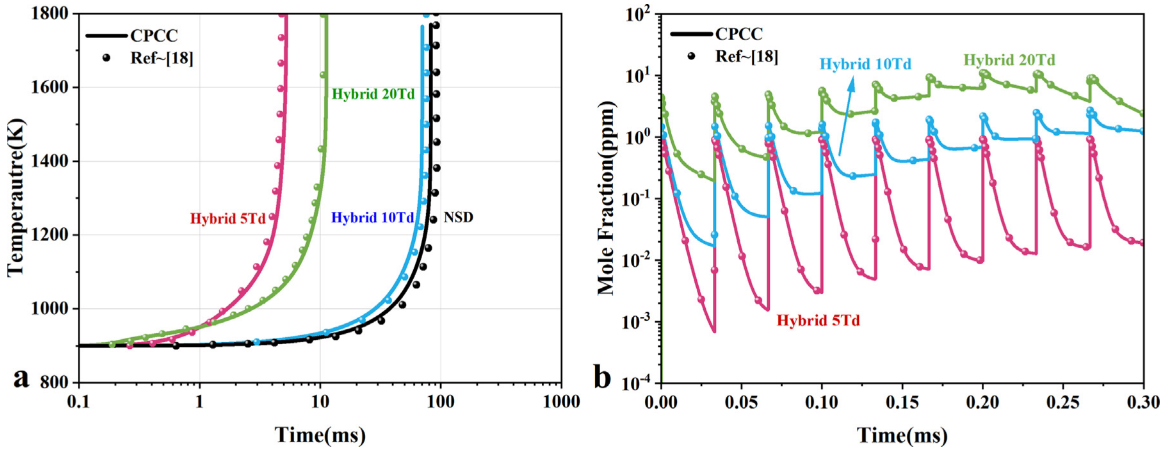

Fig. 1. Benchmark verification of the CPCC code: the temporal evolution of (a) gas temperature and (b) O density in a CH_4:O_2:He=0.08:0.17:0.75 mixture under the effect of pulsed nanosecond and DC discharges. The benchmark data are extracted from Ref. [19], the influence of the value of the E/N value in DC stage is calculated and compared directly.

$$P_{elec} = \frac{3}{2}k_B\frac{d(N_eT_e)}{dt} \tag{4}$$

$$P_{chem} = \sum_i Q_i\frac{dN_i}{dt} \tag{5}$$

where e is the unit charge, N_e is the electron number density, υ_e is the electron drift velocity, E is the electric field, T_e is the effective electron temperature and Q_i is the potential energy of species i.

The combustion chemistry process solves the equations the same as Eq. (1), and the semi–implicit ODE solver VODPK [28] is used for higher performance. Finally, gas temperature is then updated from the enthalpy of the mixture:

$$\frac{dT}{dt} = -\frac{1}{\rho\bar{c}_p}\sum_{k=1}^{K}H_k\omega_k \tag{6}$$

where T is the gas temperature, ρ is the mass density, $\bar{c}_p$ is the mean specific heat, H_k is the molar species enthalpy, and ω_k is the species molar production rates. To summarize, the plasma module and the chemistry module are calculated sequentially in one time step, the data exchange between different modules and time steps is the same as the classical hybrid plasma–combustion model proposed in Ref. [20].

The updated code used in this work is verified by reproducing the temperature and more fraction variation published in Ref. [19]. Ref. [19] discussed the effect of excitation species on ignition enhancement in CH_4/O_2/He mixture under the hybrid repetitive nanosecond and DC discharge, the updated code CPCC used in this work perfectly reproduces the results of the classical hybrid code with the same kinetics mechanism, see Fig. 1.

2.2. Chemistry mechanisms

The accuracy of the global chemistry model depends mainly on the accuracy of the chemical kinetics mechanism and the input parameters: the initial values and the time dependent E/N (reduced electric field, the electric field versus neutral density, unit in Townsend) values. In this section, we will discuss the selection of chemical kinetics mechanism for the prediction of the ignition and NO_x emission in NH_3/N_2/O_2 mixture.

The chemical kinetics schemes are composed of two parts: the plasma chemistry and the combustion chemistry. The plasma chemistry mechanism consists (i) the electron impact reactions (ionization, excitation, dissociation and attachment), (ii) the charge transfer and recombination reactions and (iii) reactions of the excited species (quenching and associative ionization):

(i) The electron impact reactions lead to the production of ions, excited species and new electrons. The elementary electron impact cross section data of nitrogen and oxygen has been well established and discussed in previous publications [29], while the cross section data of ammonia has not been provided in a complete way: there exists several data source [10,13,14] without firm validations. Thus in this work, we take the cross section data provided in two independent references, and conducted an experiment through pulsed Townsend (PT) experiments to make a direct comparison (details of the experimental setup can be found in Ref. [30]), see Fig. 2(a).

To take the advantage of the cross sections at different E/N range, we combined the cross sections from the two sources by adding ionization reactions of NH_3 from Ref. [31] into the cross section dataset proposed in Ref. [32]. As for the electron collisions with N_2, on the basis of the dataset from Lxcat [33], the cross sections of ionization reactions from Ref. [34] were added. The cross sections of attachment and dissociation reactions of O_2 from Ref. [35] were added to the cross sections from Lxcat [33].

NH_2 and NH radicals are produced efficiently via collisional dissociation of the NH_3 molecule [36]. Therefore, the electron impact reaction of NH_2 and NH is added in this study, and the cross sections are from Ref. [32] and Ref. [36]. We also consider electron impact reactions for O (from Ref. [37]), N (from Ref. [38]), H2O (from Ref. [39]) and O_3 (from Ref. [40]).

In brief, the following electron impact reactions and corresponding cross sections are considered in this work: (i)the electron impact ionization for NH_3, NH_2, NH, N, N_2, O_2, O_3, H_2O; (ii) the electron impact excitation reactions for NH_3, N, N_2, O_2, O; (iii) the electron impact dissociation for NH_3, NH_2, NH, O_2, O_3; (iv) the electron impact attachment for NH_3, NH_2, NH, O_2, O_3, H_2O.

(ii) The charge transfer reactions and recombination reactions determine the decay of electrons and ions, as well as the energy release due to these reactions. However, the information of these reactions concerning ammonia is limited: in this work, we have considered charge transfer reactions between NH_3^+, NH_2^+, NH^+ and H_2, NH_3; dissociative recombination of NH_3^+, NH_2^+ and NH^+. But the charge transfer reactions between NH_3^+, NH_2^+, NH^+ and O, O_2 are still unknown or not fully considered, the dissociative recombination of the particles under consideration may be insufficiency.

Nevertheless, this work focus mainly on the performance of plasma assisted ammonia ignition in under the effect of pulse–DC non–equilibrium plasma discharge, according to Fig. 2(b), the

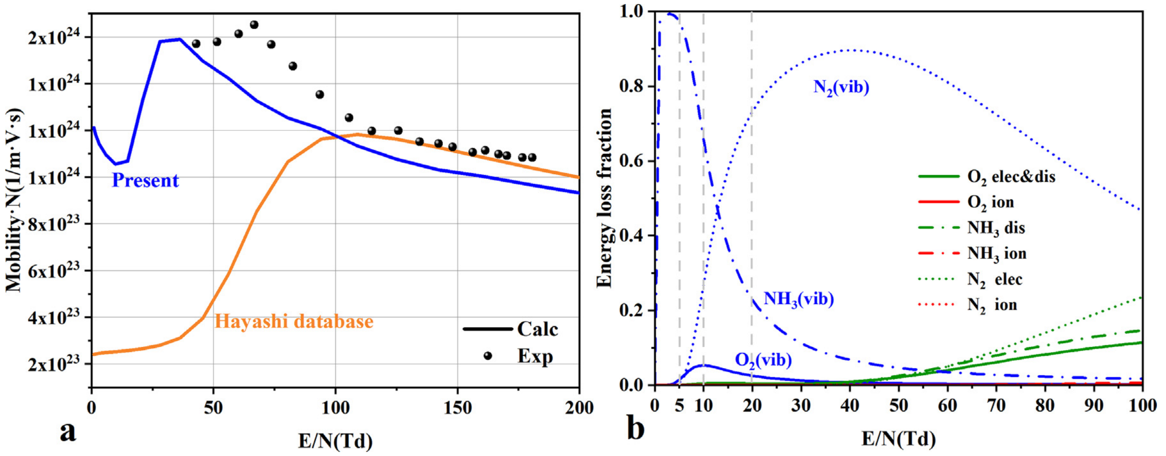

Fig. 2. Comparison of mobility of different cross sections with experimental data and energy deposition of particles in cross sections used in this study. (a) Comparison of the Mobility calculated from the cross sections used in this paper and in Hayashi database with experimental data. (b) Energy loss fraction for different reaction types as the reduced electric field (E/N) changes in the 0.219 NH_3/0.164 O_2/0.617 N_2 mixture.

electron energy goes mainly into the production of vibrationally and translationally excited states, while ions are produced only in a rather short pulse stage, thus will not greatly affect the conclusions drawn in this work.

(iii) Quenching reactions of vibrationally and electronic excited species are the key to bridge the plasma chemistry and the conventional combustion chemistry. However, the information of these reactions are also limited. A recent work [41] has evaluated the detailed electron impact reactions of ammonia molecule, but we still lack the accurate information of the rates of electronic excited NH_3 molecules reacting with other neutral species.

Thus in this work, as in previous/recent publications, we do not consider the electronic excited states of ammonia, but the role of quenching reactions of vibrationally excited species are more detailedly considered. The rates of reactions about ground state particles are taken from the work of Wang et al [42] and the chemical reactions involved in vibration-excited states are supplemented by estimation using Fridman–Macheret α-model [43]:

$$k_R(E_v,T) = AT^b exp - \frac{E_a - \alpha E_v}{RT} \vartheta(E_a - \alpha E_v) \tag{7}$$

$$\alpha \approx \frac{E_a^f}{E_a^f + E_a^r} \tag{8}$$

where k_R, E_a, E_v and ϑ represent the rate constant of the reaction, the potential energy of the vibratory excited state, the efficiency with which the vibratory excited state reduces the activation energy of the reaction, the Heaviside function (when E_a is greater than 0, $\vartheta(E_a - \alpha E_v) = 1$; When E_a is less than 0, $\vartheta(E_a - \alpha E_v) = 0$, respectively. E_a^f and E_a^r represent activation energy for forward reaction and that for backward reaction, respectively. Relaxations and vibrational–vibrational (V–V) interactions of $N_2(v)$ and $O_2(v)$ are the same as Mao et al. [44], mainly from Capitelli et al. [45] and Starikovskiy et al [6].

The combustion chemistry of $NH_3/N_2/O_2$ mixture has been studied quite intensively in the past years. Various set of mechanisms have been proposed, e.g. the MEI mechanism, [46], the OTO mechanism [47], the GLA mechanism [48] and the CEU mechanism [42]. MEI, OTO, and GLA mechanisms are close to the experimental data in the comparison of ignition delay time at an initial temperature of 298 K by Taneja et al [14]. CEU mechanism is a newer and simplified mechanism, so it is also included as a candidate for the combustion mechanism. The final choice of combustion mechanism will be discussed later in Section 2.3.

2.3. Performance of the chemistry mechanisms

The performance of plasma and combustion chemistry mechanisms are checked and evaluated in this section, respectively.

The plasma chemistry mechanism proposed in Section 2.2 is checked by making a direct comparison on the temporal evolution of gas temperature and NH_3(v2) density with those presented in Ref. [14], keeping the same combustion chemistry (Ref. [46]), see Fig. 3. With the same working conditions (30 kHz, 150 Td NS discharge at an initial temperature of 1500 K), the plasma chem-

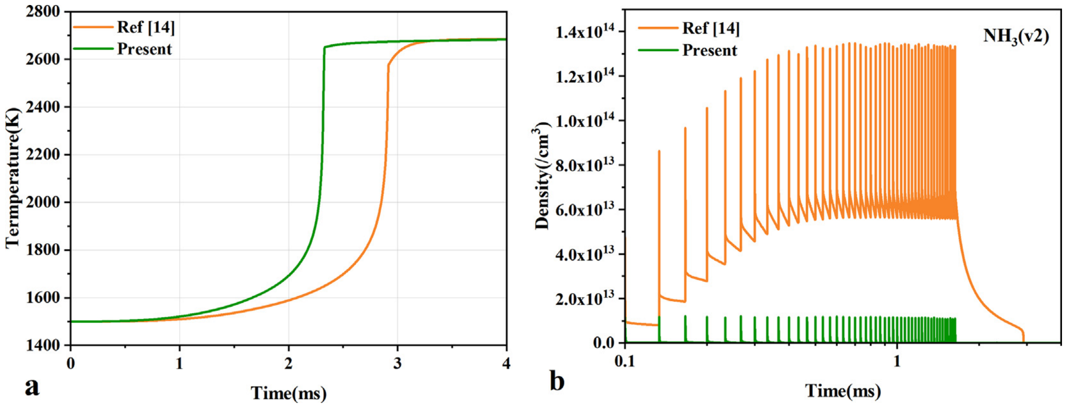

Fig. 3. Comparison between new mechanism and Taneja's mechanism of (a) gas temperature and (b) density of NH_3(v2) using the same combustion mechanism and working condition. The calculation conditions are as follows: initial temperature 1500 K, constant pressure 1 atm, 50 square wave pulse discharges with frequency of 30 kHz at 150 Td.

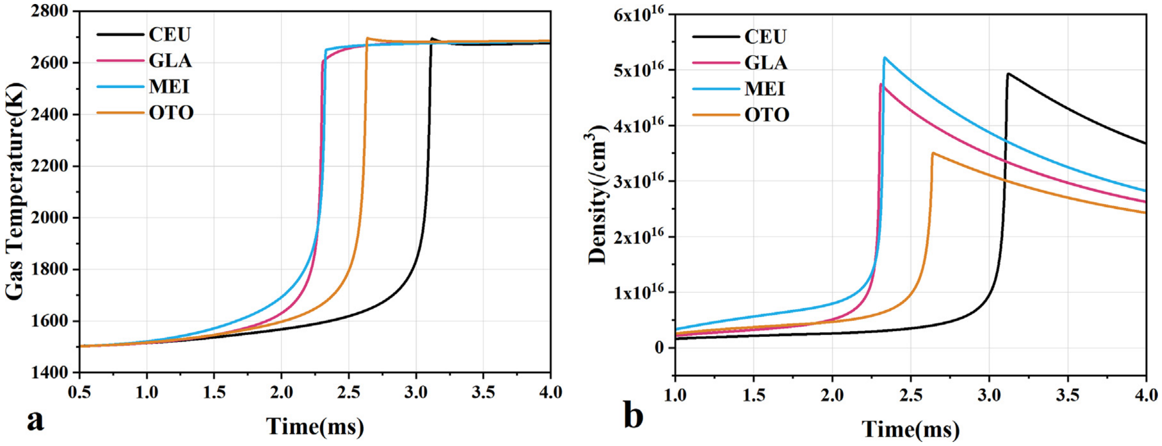

Fig. 4. Comparison of the effects of 50 pulses on systems with different mechanisms under the condition of stoichiometric mixture, reduced electric field of 200 Td, frequency of 30 kHz, initial temperature of 1500 K and 1 atm pressure. (a) Temperature changes over time (b) The variation of NO density.

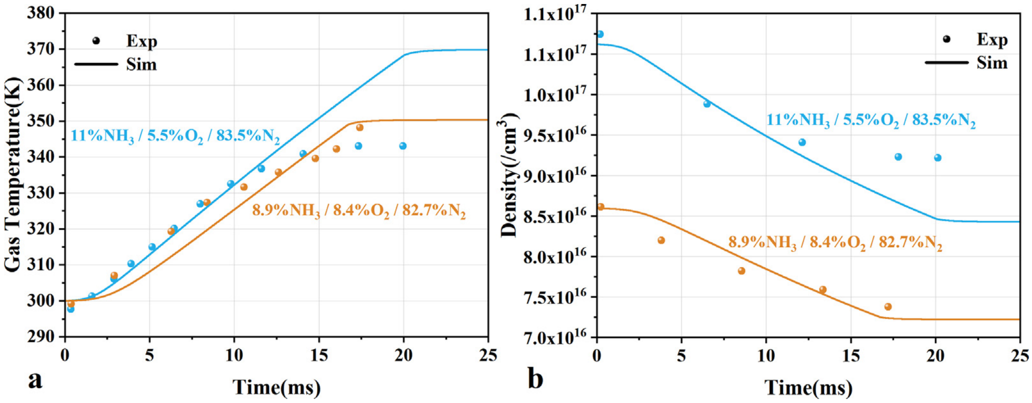

Fig. 5. Comparison between experimental and simulated results of (a) gas temperature and (b) NH_3 density of $NH_3/O_2/N_2$ mixtures.

istry mechanism proposed in this work leads to a faster temperature rise and a smaller ignition delay time (Fig. 3(a)), and the NH_3 density is much lower, as shown in Fig. 3(b). This is because more $NH_3(v)$, $O_2(v)$ and $N_2(v)$ reactions have been extended to the plasma chemistry mechanism in this work.

The combustion chemistry mechanism is chosen by comparing the calculated evolution of gas temperature and NO density under the influence of the NS discharges using different combustion mechanisms, keeping the same plasma chemistry proposed in this work. With the same working conditions (50 pulses under the condition of stoichiometric mixture, reduced electric field of 200 Td, frequency of 30 kHz, initial temperature of 1500 K and 1 atm pressure), the calculated temperature rise and NO density are shown in Fig. 4(a) and (b).

It is clearly seen that the GLA and MEI mechanism is close to each other in both ignition delay time, while the OTO and CEU mechanisms predict slower ignition. It has to be noted that, Ref. [14] has reviewed the GLA, MEI and OTO mechanisms in ignition delay time by making comparisons with rapid compression machine experiments, and concluded that their performance are close to each other. However, in presence of plasma chemistry, the performance of the MEI and GLA schemes are still close while the OTO differs a lot.

The predicted NO density by MEI and GLA mechanisms are also close while the OTO mechanism gives a significantly lower density than the other three mechanisms, as is shown in Fig. 4(b). We prefer the MEI and GLA mechanisms, which provide rather similar NO production and ignition delay time. As size of the GLA mechanism is smaller than MEI, the GLA mechanism was used for higher computational speed.

To verify the mechanism, a direct comparison of gas temperature and NH_3 density evolution with the experimental data from Ref. [15] and Ref. [17] has been conducted. As is shown in Fig. 5, a good agreement is achieved for the $0.089NH_3/0.084O_2/0.827N_2$ mixture, while for the case of $0.11NH_3/0.055O_2/0.835N_2$ mixture, the predicted equilibrium gas temperature is slightly higher, thus the NH_3 density is lower than the measurement. This discrepancy may caused by (1) the inconsistently given E/N value or (2) the increased portion of NH_3 (the electron impact cross sections of NH_3, is still incomplete till now)

To summary, the chemistry mechanism used in this work is a combination of plasma and combustion chemistry. The proposed mechanism consists of 582 plasma reactions and 218 combustion chemical reactions, totally 80 species are considered in this mechanism.

2.4. *E/N definition and initial conditions*

A fit to the experimental process temperature by Lefkowitz et al. [20] reveals that E/N of 200 Td is achievable in DBD discharges. The inter-pulse DC discharge E/N of 0–20 Td can be achieved by maintaining a DC voltage value (lower than the ionization threshold) between pulses, this low and constant reduced electric field has been proved to be able to effectively promote the generation of electron excited state particle $O_2(a^1\Delta_g)$ which contributes significantly to ignition [18,19]. The waveform of the reduced electric field E/N studied in this work therefore is set as 200 Td during the NS pulse stage and 5–20 Td during the DC stage (see Fig. 6) and the discharge frequency is 50 kHz. In the following

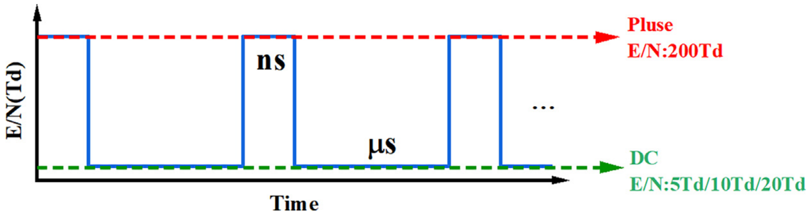

Fig. 6. The temporal evolution of E/N as inputs used in this work. The energy deposition of each pulse is fixed, so the time of each pulse is slightly different. DC discharge occurs from the end of the pulse to the beginning of the next pulse.

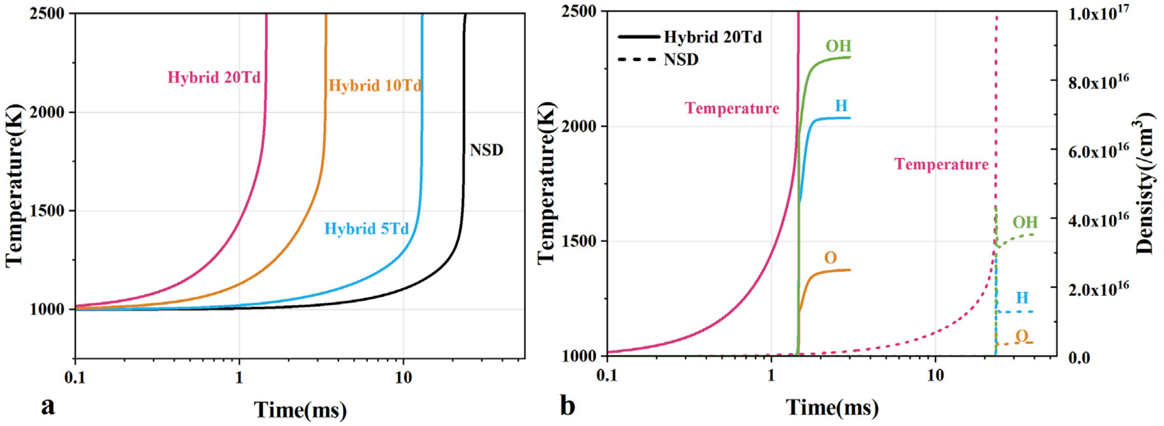

Fig. 7. (a) Variation of temperature under different E/N values of DC discharge. (b) The change of temperature and density of O, H and OH in different systems with time.

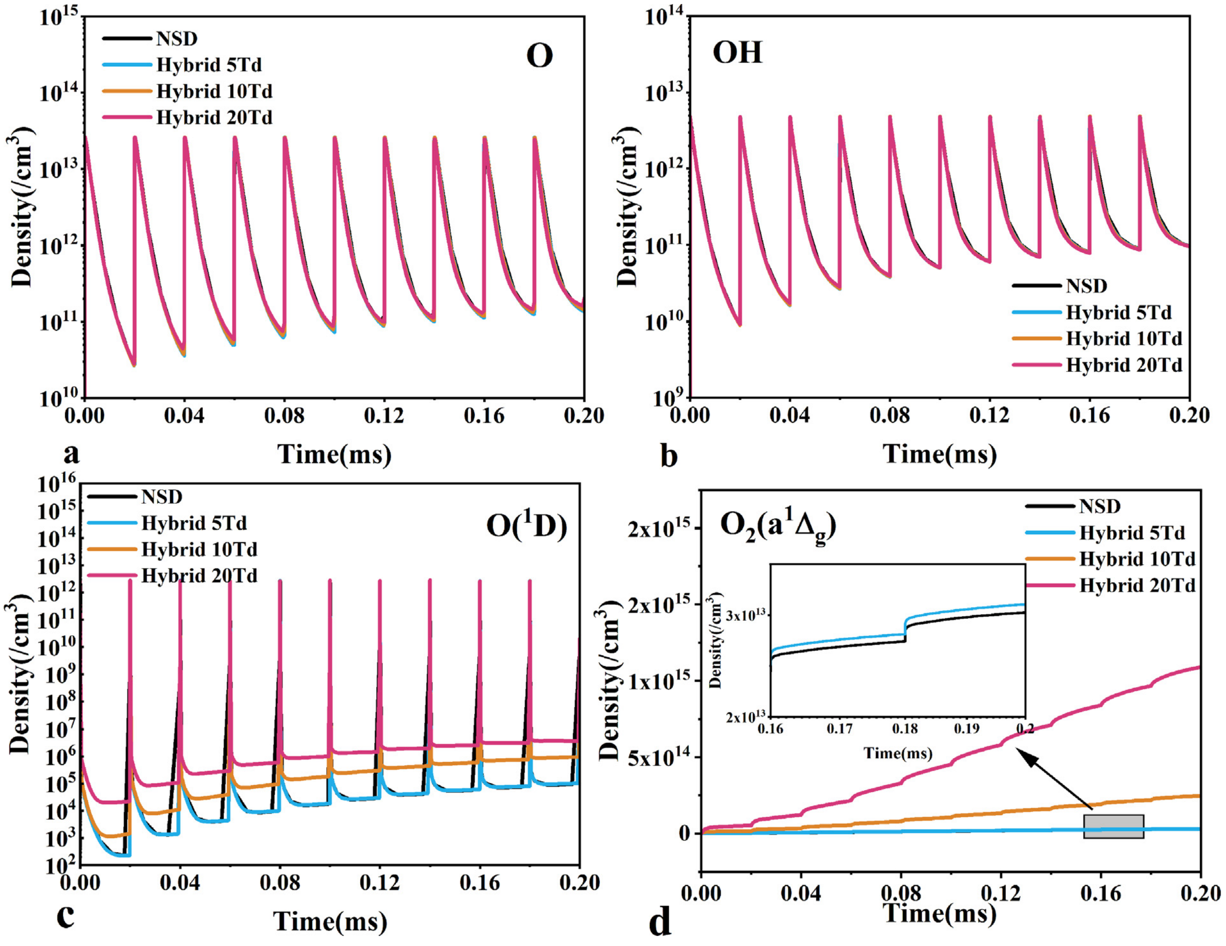

Fig. 8. Time evolution of (a) O, (b) OH, (c) O(^{1}D) and (d) $O_2(a^1\Delta_g)$ in the first 10 pulses under different DC E/N values.

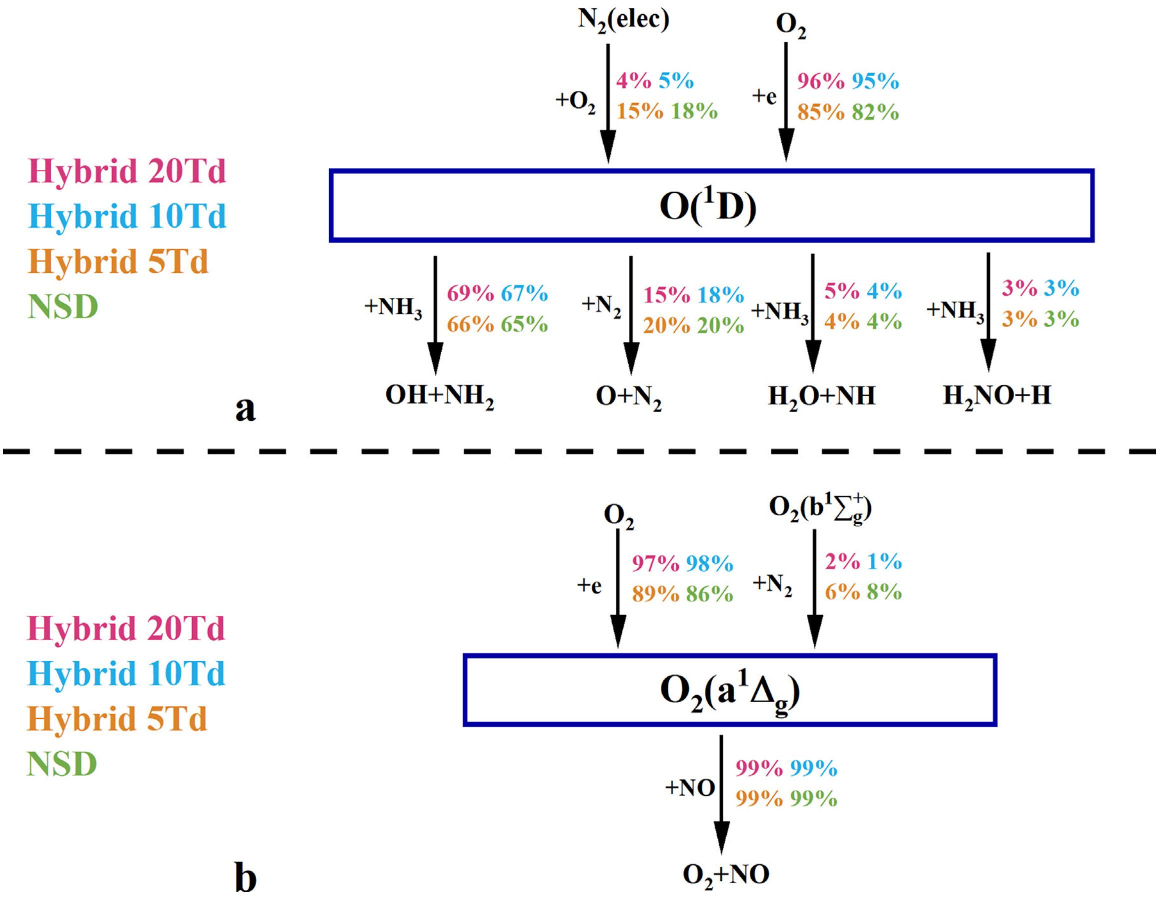

Fig. 9. The (a) $O(^1D)$ and (b) $O_2(a^1\Delta_g)$ path flux analysis at hybrid 0–20Td.

text, we denote “NSD” as nanosecond pulsed discharges, “Hybrid” as coupled nanosecond pulsed and DC discharges.

The energy deposition of each pulse set as the same 5×10^{-5}J/cm^{-3}. All systems are adiabatic and at a constant pressure of 1 atm. The component concentration was set according to the stoichiometric mixture of $0.219NH_3/0.164O_2/0.617N_2$. The initial temperature was set as 1000 K. The fuel is considered to be ignited when the gas temperature reaches 2500 K and the discharge stops at the moment the gas temperature reaches 2500 K.

3. Results and discussion

3.1. The role of key species on the ignition delay time of the NH_3/air mixture driven by hybrid pulse–DC discharges

High ignition energy threshold is one of the key factors limiting the applications of NH_3 as a fuel. By coupling a constant electric field (DC discharge) during the gap of NS discharges, as shown in Fig. 7(a), the existence of DC fields between pluses can significantly reduce the ignition delay time by 1 orders of magnitudes, this is in consistent with previous studies conducted in $CH_4/He/O_2$ mixture [19] and $H_2/O_2/He$ mixture [18]. In order to exclude the influence of different energy deposition at the DC stage, we plotted the energy deposition curves of the mixture under different conditions (see supplementary materials). The total energy deposition at hybrid 20Td is about 8 times that at NSD, so the addition of DC discharge is not a simple increase in energy deposition to enhance ignition. And the introduction of DC stage brings another interesting phenomenon, as shown in Fig. 7(b): the sharp increase of temperature appears 0.4–0.6 ms earlier than the moment H, OH or O rise, while in case there are only NSD stages, the temperature and typical species density are rising almost at the same time moment.

To investigate, in presence of the DC stage, the reason of ignition delay reduction as well as time shift between temperature rise and density rise, the role of key radicals and excited species: O, OH, $O(^1D)$,$O_2(a^1\Delta_g)$, $NH_3(v)$ and $O_2(v)$ are analyzed.

The evolution of O and OH density are calculated and displayed in Fig. 8(a) and (b): it is clearly seen that hybrid DC discharge has no significant influence on O and OH density, thus O and OH are not the main reasons for the reduction of ignition delay time.

The important excited state particle, $O(^1D)$, has a strong kinetic effect on ignition (Ref. [18,19]). Although hybrid DC discharges can increase the concentration of $O(^1D)$ (Fig. 8(c)), it does not have an effect on its main consumption pathway (Fig. 9(a)). 80% of $O(^1D)$ reacts with NH_3 and removes the hydrogen atom from NH_3, which is a strong kinetic enhancement.

The concentration of $O(^1D)$ increases with the E/N value of DC stage. From Fig. 9(a) it can be seen that at hybrid 10 Td or 20 Td DC discharge, the $O(^1D)$ generated by electron collision is approximately 1–2 orders of magnitude more than the other systems. This means that at E/N of 10 Td or 20 Td, electrons are more likely to collide with O atoms to produce more $O(^1D)$.

The density of $O_2(a^1\Delta_g)$ in the NH_3/air mixture increase significantly with the increase of E/N in the DC stage in merely 10 pulses (within 0.1 ms), as shown in Fig. 8(d). A path flux analysis of $O_2(a^1\Delta_g)$ shows that almost all $O_2(a^1\Delta_g)$ is produced by the collisional excitation of electrons with O_2, with a small amount produced by the quenching of $O_2(b^1\Sigma_g^+)$, see Fig. 9(b).

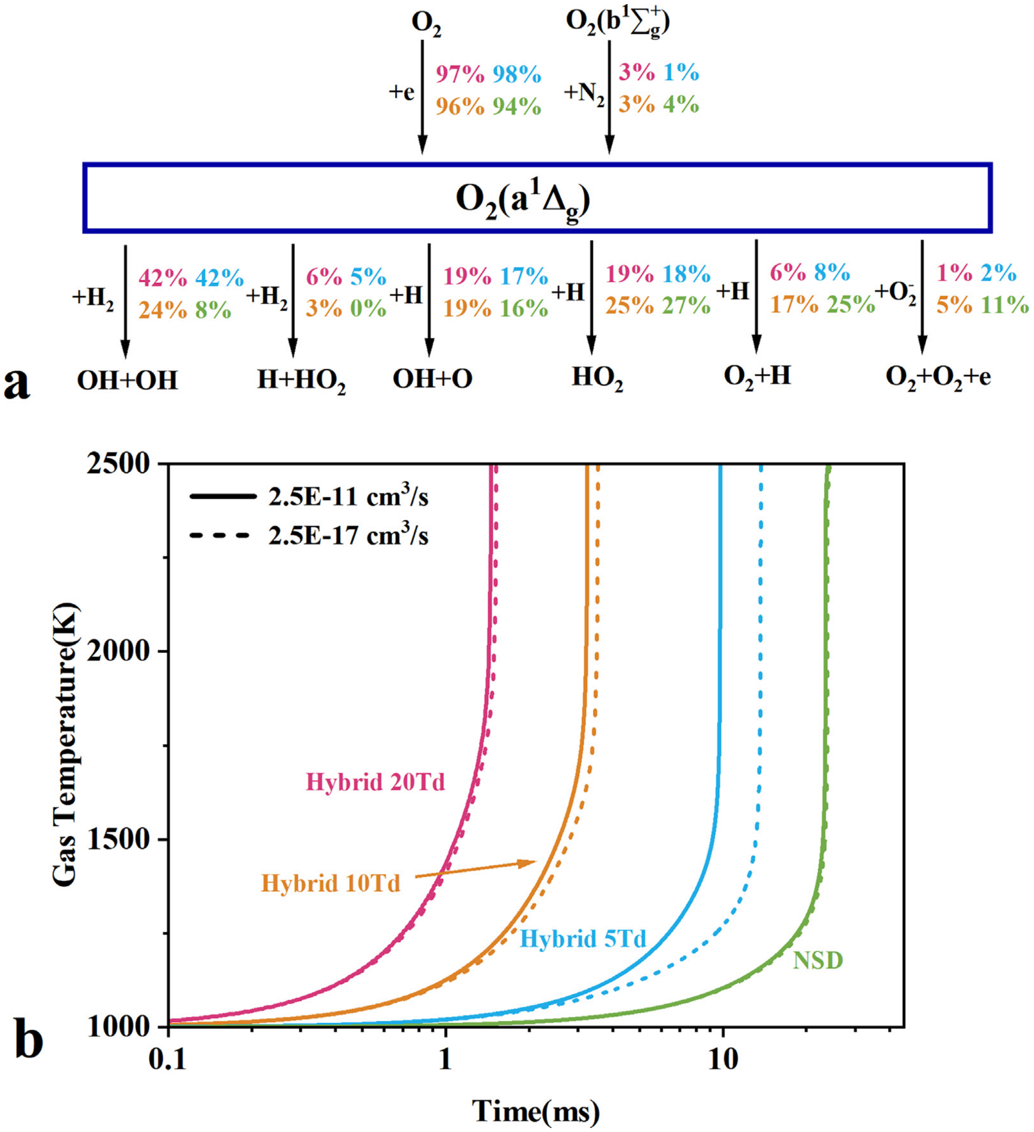

Fig. 10. (a) Path analysis of $O_2(a^1\Delta_g)$ using correct reaction rate constant of $NO + O_2(a^1\Delta_g) \rightarrow NO + O_2$. (b) Time evolution of gas temperature using different rate constant of $NO + O_2(a^1\Delta_g) \rightarrow NO + O_2$ at hybrid different E/N values of DC discharges.

The role of $O_2(a^1\Delta_g)$ in ignition has been well emphasized in previous studies, due to its relative long life time and high reaction rates with H atoms and CH_3 radicals [19]. However in the mixture of NH_3/air studied in this work, we do not observe the significant enhancement of reaction pathway $NH_2 + O_2(a^1\Delta_g) \rightarrow$ product or $H_2 + O_2(a^1\Delta_g) \rightarrow$ product, instead, the majority of $O_2(a^1\Delta_g)$ is consumed in reactions with NO (see Fig. 9(b)).

The reaction rate constant of $NO + O_2(a^1\Delta_g) \rightarrow NO + O_2$ used in this study is the same as most fuel/air mixture plasma–assisted combustion mechanisms, which is $2.5 \times 10^{-11} cm^3/s$. However, it was found that this is a typo in Ref. [49]. The rate constant of this reaction was measured in a number of works and its rate constants should be $2.5 \times 10^{-17} cm^3/s$ (see, for example, Ref. [50,51]).

Using the correct rate constant, we recalculate the ignition process. In the new results (see Fig. 10(a)), $O_2(a^1\Delta_g)$ no longer quenched with NO. Instead, it shows a strong kinetic effect: 8%–48% reacts with H_2 and 44%–68% reacts with H. In addition, with the correction of the reaction rate constant, the ignition delay at hybrid DC discharge is also reduced, especially at hybrid 5Td (decreases from about 14ms to less than 10ms, see Fig. 10(b)). This means mechanisms using the wrong rate constant will underestimate the enhancement of $O_2(a^1\Delta_g)$ on ignition. Since most of the current research based on pulse discharge or there's not a lot of NO in the mixture, this problem is not obvious. However, when calculating the discharge of low reduced electric field for a long time and the mixture contains a lot of NO (e.g. gliding arc assisted NH_3/Air ignition), the wrong rate constant will cause obvious influence on $O_2(a^1\Delta_g)$'s role in ignition enhancement and ignition delay.

In addition, water molecules take 20–25% of the total molecules and it was reported in Ref. [52] that hydrated negative ions (e.g. $O_2^-(H_2O)_n$) can reduce the efficiency of the mechanism of primary electron production. It can also affect the density of O_2^-, species which accounts for 1–11% of $O_2(a^1\Delta_g)$'s consumption. To study the effects of hydrated negative ions, the authors added reactions of hydrated negative ions from Refs. [52] and [53] (e.g. $O_2^- + H_2O + M \rightarrow O_2^-(H_2O) + M$).

A pulse–DC (200Td pulse stage and 20Td DC stage) case is calculated, results show that, hydrated ions significantly affect the

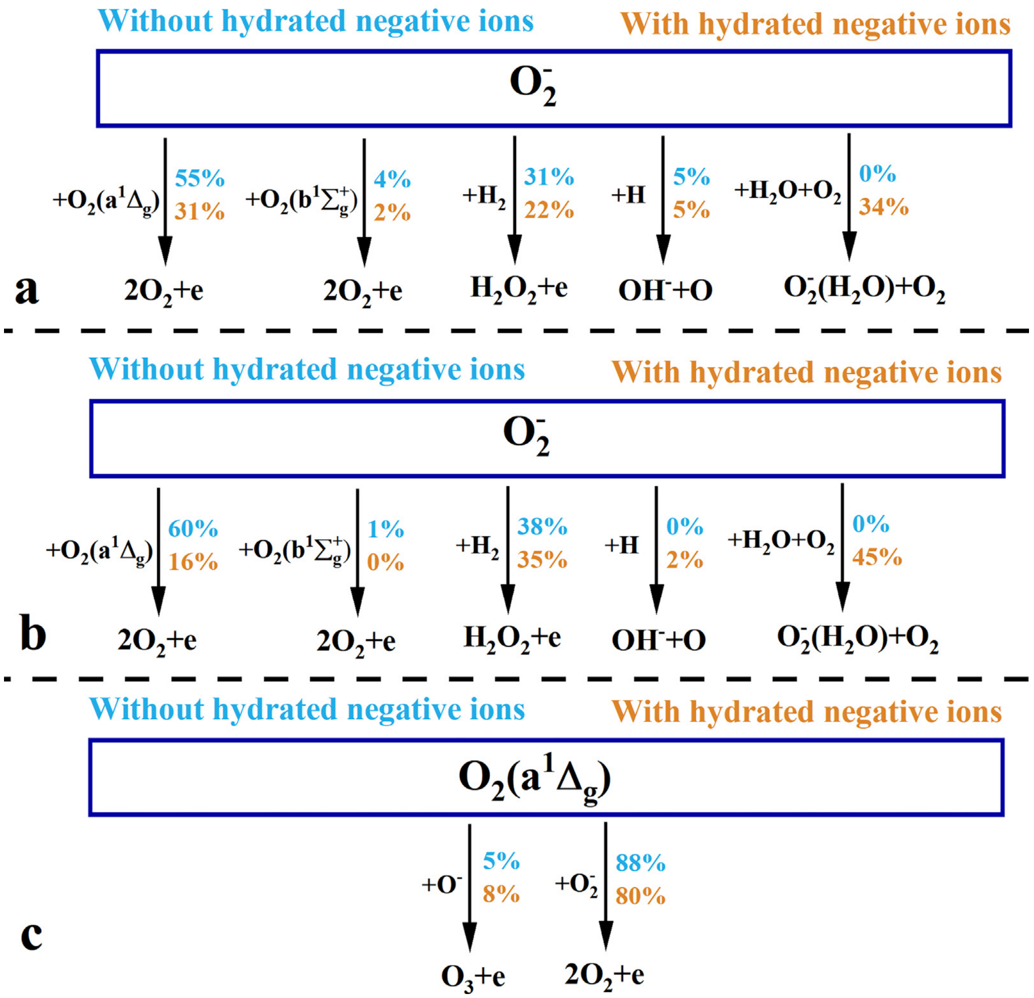

Fig. 11. Consumption path flux analysis of O_2^- and $O_2(a^1\Delta_g)$ before and after adding hydrated negative ions. The discharge mode is pulse hybrid 20Td DC discharges. (a) Consumption path analysis of O_2^- in 0–0.1 ms. (b) Consumption path analysis of O_2^- in 0.4–0.5ms. (c) Consumption path analysis of $O_2(a^1\Delta_g)$ in 0–0.1 ms.

evolution of O_2^- and $O_2(a^1\Delta_g)$, as can be seen in the following figure: 34% to 45% O_2^- are consumed in the reaction with water molecule (see Fig. 11(a,b)), as a result, only 80% (originally 88% without considering hydrated negative ions) $O_2(a^1\Delta_g)$ are quenched through $O_2^- + O_2(a^1\Delta_g) \rightarrow 2O_2 + e$ during 0–0.1 ms (see Fig. 11(c)).

The changes of the reaction path due to the presence of hydrated negative ions lead to a sharp reduction of electrons, thus all the electron impact reactions change, the predicted temperature is too low when comparing with experimental data. The authors have not find a solution to the problem of the low predicted temperature. A detailed analysis has been attached in the supplemental material.

NH_3 and O_2 are species present in large quantities in NH_3/air mixture and according to Fig. 2(b), their vibrationally excited state particles are produced in large quantities during the DC discharge stage, so the promotion of ignition by the excited state particles of these two particles, $NH_3(v2)$ (NH_3 in other vibrationally excited states has a very low concentration due to low energy deposition) and $O_2(v1)$, needs to be studied.

Figure 12(a) shows the evolution of $NH_3(v2)$ density during the first 10 discharge pulses. With the increase of E/N in DC stages from 0 to 20 Td, the density of $NH_3(v2)$ increase by 100 times from $10^{12}\,cm^{-3}$ to $10^{14}\,cm^{-3}$. $NH_3(v2)$ will affect the process of ignition mainly through heat released from V–T (Vibration–Translation) relaxation, as is shown in Fig. 12(b), with or without DC stages, 99% of $NH_3(v2)$ is quenched by ground state ammonia molecule:

$$NH_3(v2) + NH_3 \rightarrow 2NH_3 \tag{R1}$$

The hybrid DC discharge contributes significantly to the production of $O_2(v1)$, as is shown in Fig. 13(a). With the increase of E/N in DC stages from 0 to 5 Td, the density of $O_2(v1)$ increase by 1 order of magnitudes, from 5 Td to 10 Td 2 orders of magnitude while from 10 Td to 20 Td, the density increase just by 2 times: the fraction of electron energy dissipated into $O_2(v1)$ peaks between 5–10 Td, in correlation with Fig. 2.

A path flux analysis shown in Fig. 13(b) indicates that, $O_2(v1)$ are consumed through V–T, V–V relaxations and reactions with H atoms. Without DC stage, 99% of $O_2(v1)$ are consumed in the V–T reaction:

$$O_2(v1) + O_2 \rightarrow 2O_2 \tag{R2}$$

The increase of E/N value in the DC stage leads to the increase rate of V–V reactions:

$$O_2(v1) + O_2(v1) \rightarrow O_2 + O_2(v2) \tag{R3}$$

$$O_2(v1) + O_2(v2) \rightarrow O_2 + O_2(v3) \tag{R4}$$

It means that the majority of vibrationally excited oxygen molecules contribute to ignition through heat release from V–T relaxation.

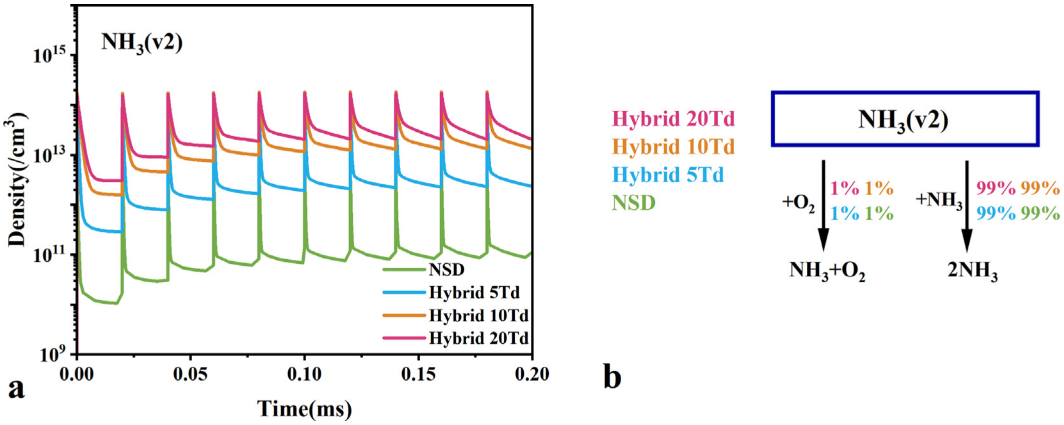

Fig. 12. Evolution of NH_3(v2) density and its path analysis. (a) Changes in NH_3(v2) density in different systems during the first 10 pulses. (b) Analysis of consumption path fluxes of NH_3(v2) from the beginning of the reaction to the moment of ignition.

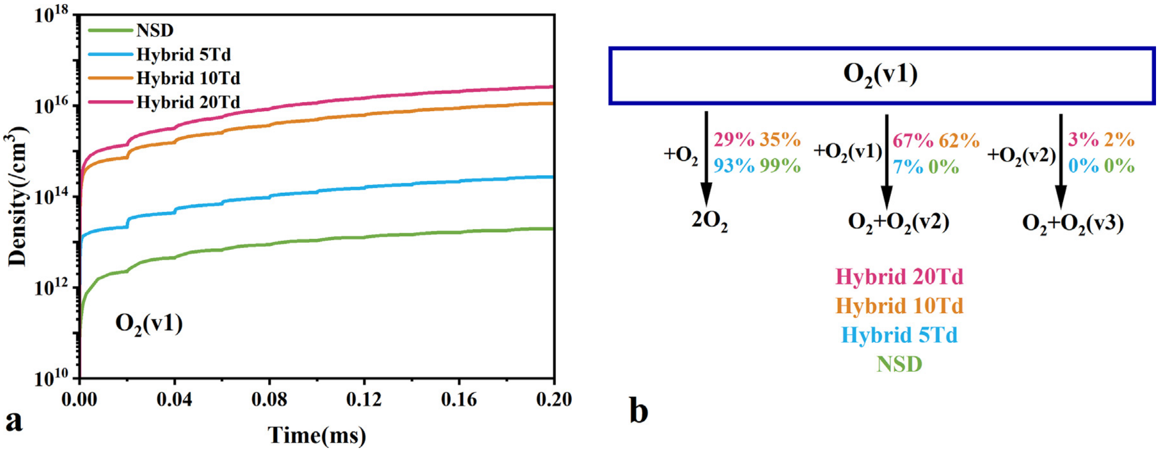

Fig. 13. Evolution of O_2(v1) density and its path analysis. (a) Changes in O_2(v1) density in different systems during the first 10 pulses. (b) Analysis of consumption path fluxes of O_2(v1) from the beginning of the calculation to the moment of ignition.

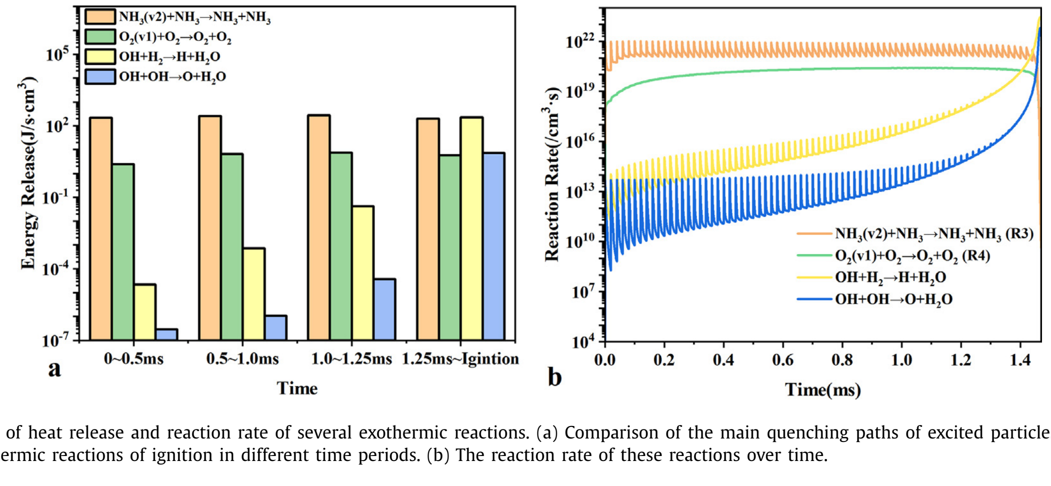

Fig. 14. Comparison of heat release and reaction rate of several exothermic reactions. (a) Comparison of the main quenching paths of excited particles NH_3(v2) and O_2(v1) with the main exothermic reactions of ignition in different time periods. (b) The reaction rate of these reactions over time.

We have found that the role of NH_3(v2) and O_2(v1) species in NH_3/air mixture driven by Pulse–DC discharge (in range of E/N=0–20 Td) prior to ignition is thermal effects due to quenching reactions. The quantitative values of energy release from these reactions are calculated and compared with main exothermic reactions of conventional combustion processes, see Fig. 14(a). Energy release from NH_3(v2) through (R1) dominates before 1.25 ms, until the early stage of ignition, $OH + H_2 \rightarrow H + H_2O$ starts to take the main role. Throughout the discharge–ignition period, the heat release from O_2(v1) and $O_2(a^1\Delta_g)$ is much lower than

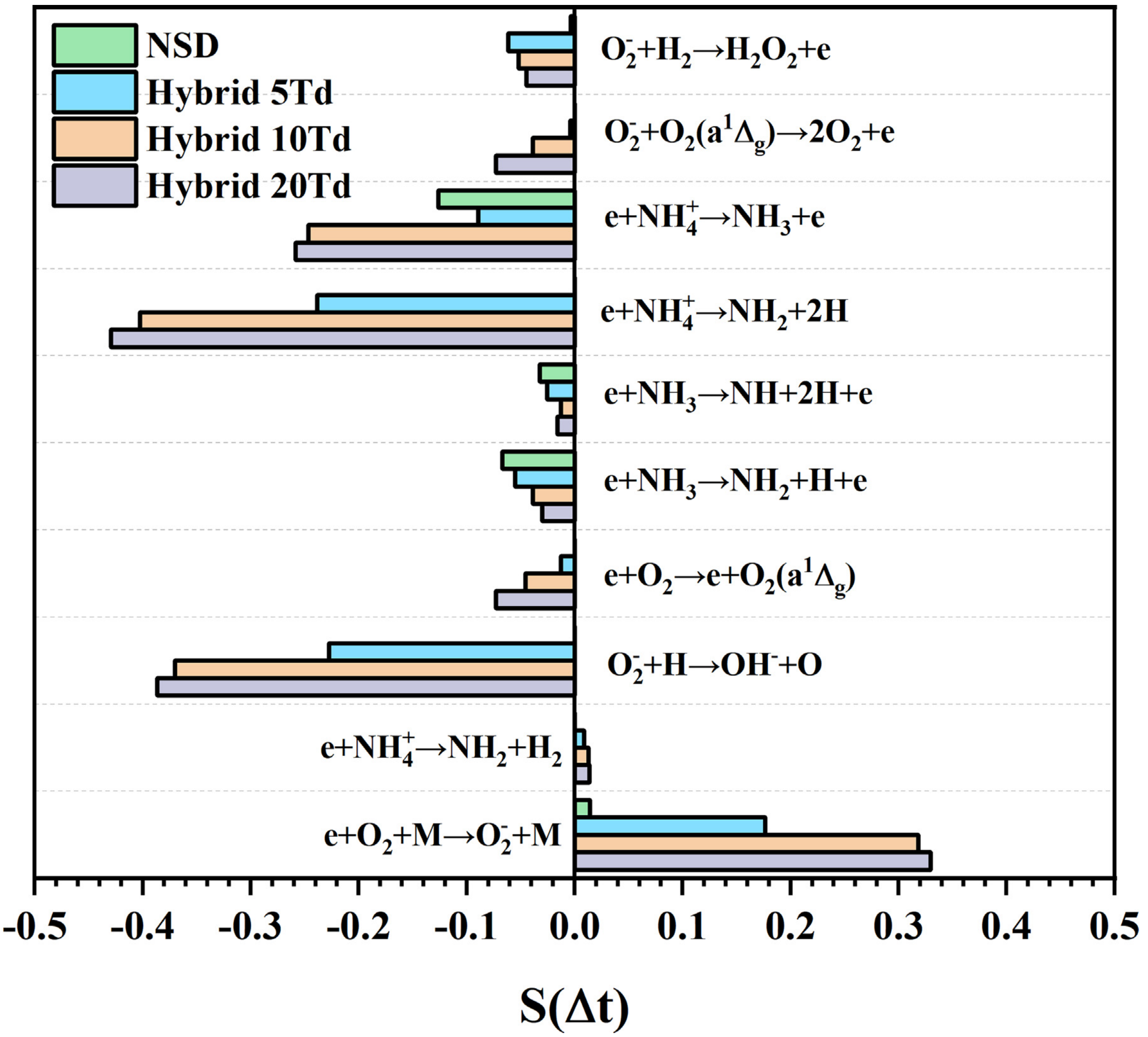

Fig. 15. Sensitivity analysis of ignition delay times about plasma chemistry reactions, $S\Delta(t) = \frac{\tau(2rrt(i))-\tau(rrt(i))}{\tau(rrt(i))}$ (τ and rrt(i) represent the ignition delay time and reaction rate of the ith reaction respectively).

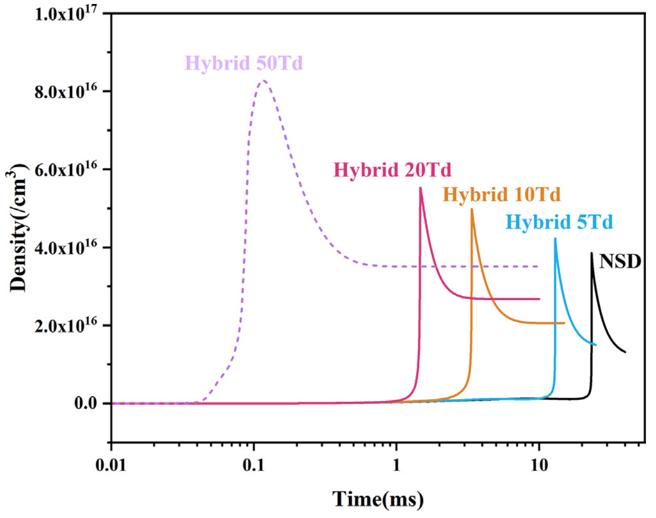

Fig. 16. Time variation curve of NO density in the whole process under NSD coupling with DC discharge of different values.

that of NH_3(v2): the quenching reaction rate of (R1) approaches $10^{21}/\mathrm{cm}^3 \cdot s$, 2 orders of magnitudes larger than that of (R2), see Fig. 14(b).

Finally a sensitivity analysis was carried out to find the key reactions affecting the ignition delay time, the results are plotted in Fig. 15.

The following detachment reactions of O_2^- promote the production of electrons in the DC stage:

$$O_2^- + H_2 \rightarrow H_2O_2 + e \tag{R5}$$

$$O_2^- + O_2(a^1\Delta_g) \rightarrow 2O_2 + e \tag{R6}$$

The ignition delay is most sensitive to (R6) when E/N= 10–20 Td in DC stages due to higher $O_2(a^1\Delta_g)$ production rate. The presence of high density electron allows the following reactions producing excited molecules, thus reducing the ignition delay time.

Other key reactions, including electron impact dissociation reaction of NH_3 ($NH_3 + e \rightarrow 2H + NH + e$, $NH_3 + e \rightarrow H + NH_2 + e$), electron impact ionization and excitation reaction also benefit the ignition of by providing radicals (NH, NH_2 and H), electrons or chemically active species ($O_2(a^1\Delta_g)$).

The charge transfer reaction $O_2^- + H \rightarrow OH^- + O$ also has an positive effect on the ignition delay time, as O atoms are more effective than H atoms in promoting ignition via NS hybrid DC discharges.

In contrast, the following electron consuming reactions (attachment and dissociative recombination reactions) inhibit

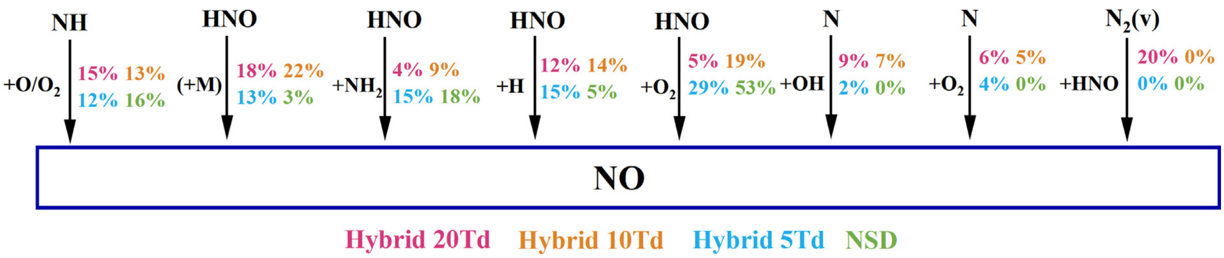

Fig. 17. Analysis of NO production path fluxes.

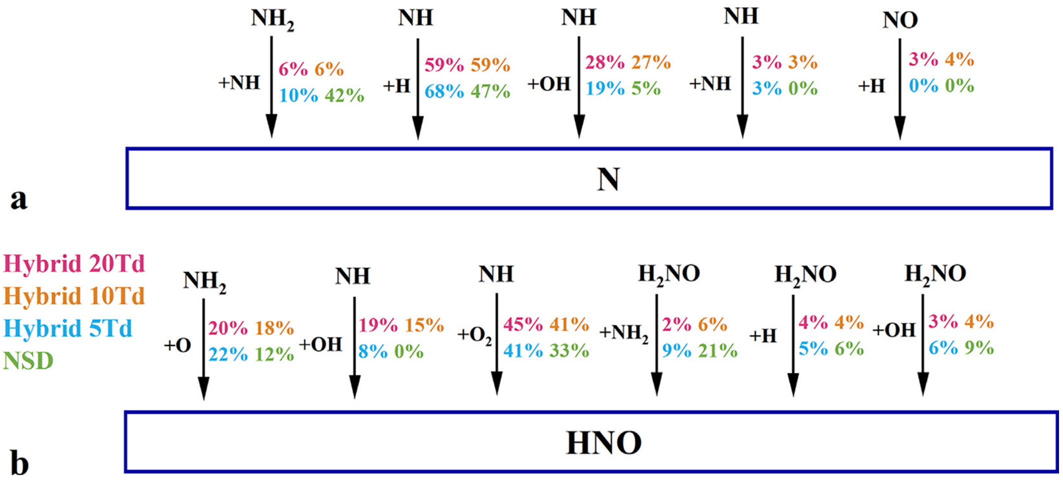

Fig. 18. Flux analysis of the pathway for the production of (a) N and (b) HNO.

the ignition:

$$e + 2O_2 \rightarrow O_2^- + O_2 \tag{R7}$$

$$e + NH_4^+ \rightarrow NH_2 + H_2 \tag{R8}$$

3.2. *Effects of NS-coupled DC discharge on* NO *compared with NS discharge*

NO_x has been an important indicator for monitoring exhaust gases and has been a main concern in applications related with ammonia combustion. NO is an important particle in the production of NO_x: Most of the NO_x generated directly from combustion is NO and it will be oxidized to produce NO_x after emission. In this section we take NO as a "marker", study the features of the NO_x emission in NH_3/air combustion system affected by pulse–DC discharges.

Figure 16 shows the evolution of NO density before and after ignition, driven by different E/N values in DC stage. The concentration of NO varies in the order of 10^{16} cm^{-3}, and will increase with the E/N value at DC stage. The NO concentration at hybrid 20 Td is nearly twice as that driven by NSD, an additional calculation with higher E/N (50 Td) in the DC stage (the dotted line) indicates that the NO density has an upper limit around $4 \times 10^{16} cm^{-3}$.

The production of NO can be understood from the flux analysis shown in Fig. 17: NO originates mainly from NH (12–16%), HNO (39–58%), N (0–15%) and N_2(v) (0–20%) and there's no direct connection to $O_2(a^1\Delta_g)$.

The percentage of NO generated from NH is basically the same for all four systems, while the contribution from HNO related reactions varies significantly with E/N: the percentage of NO produced from HNO decreased from around 58% to 39% when the E/N in DC stage increased from 5 to 20 Td. Despite the decreasing fraction of contribution from HNO, the absolute amount of NO generated from HNO changes little (from $2 \times 10^{16} cm^{-3}$ to $3.6 \times 10^{16} cm^{-3}$): the multiplication between Figs. 16 and 17 indicates that, the peak NO density by the percentage of NO produced by HNO and peaks at E/N = 5–10 Td.

N_2(v) and N play important roles in NO production when E/N in DC stages exceeds 10 Td, due to the increasing contribution of following reactions:

$$N + OH \rightarrow NO + H \tag{R9}$$

$$N_2(v) + HNO \rightarrow NO + NNH \tag{R10}$$

In summary, the main sources of NO at NS hybrid DC discharges are N, HNO and N_2(v). In order to study whether the rapid increase of NO caused by hybrid DC discharge is unique to NH_3/air mixture or exists in the air-containing mixture, we conducted path analysis for species which are the main sources of NO, see Fig. 18. 45%–97% of HNO and nearly 100% of N come from NH and NH_2. The NO produced by NH, N and HNO accounted for 80%–99% of the total NO production, and these species were all from NH_3–related–particles. This assures that, the rapid increase of NO is unique in the NH_3/air mixture, this is one of the key differences with the kinetics in hydrocarbon based fuel–air mixtures.

The path flux analysis of NO consumption is shown in Fig. 19. At low DC E/N values (0–5 Td), the majority of NO are consumed by colliding with NH and NH_2 molecules (91–94%), leading to the production of H, OH and NNH radicals. At higher DC E/N values (10–20 Td), the contribution of those reaction channels drops to 78–83%, the influence of N and HO_2 becomes significant.

The change of reaction channels of NO at low and high DC E/N values can be explained by plotting the evolution of NO, NH_2, NH density and gas temperature together at different DC E/N values (see Fig. 20): it is clearly seen that, in case of higher DC E/N value (20 Td), NH and NH_2 density drop before NO density peaks while for NSD discharges, NH and NH_2 density increase together with NO density.

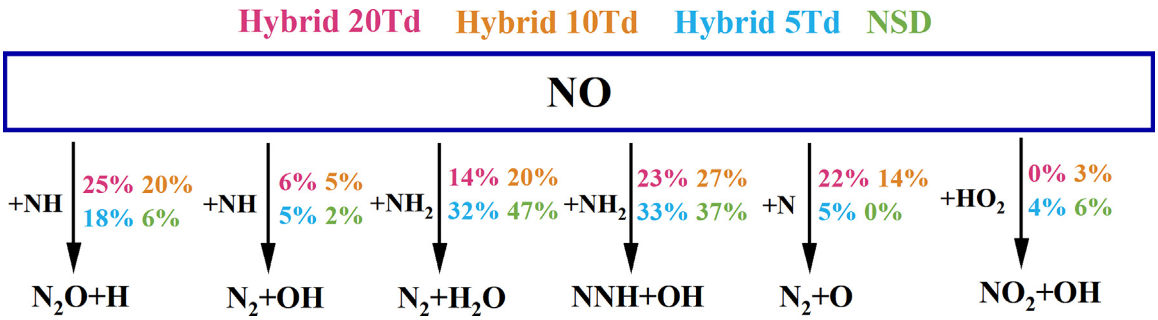

Fig. 19. Analysis of NO consumption path fluxes.

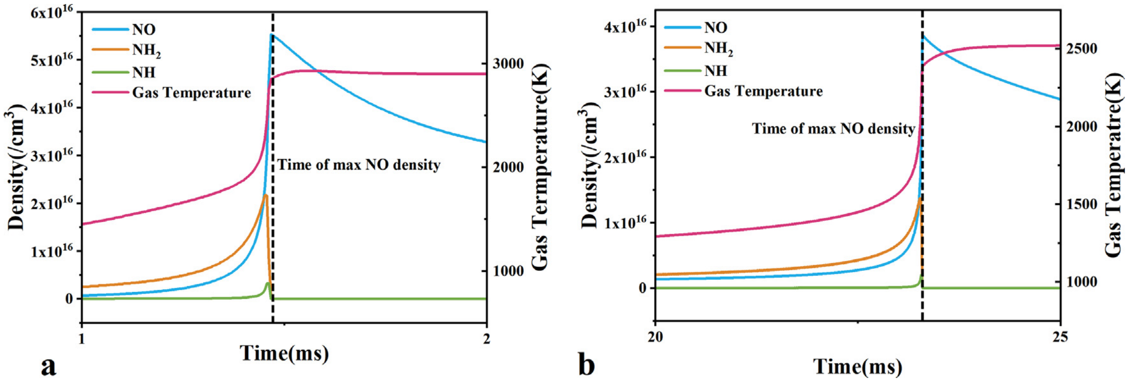

Fig. 20. The changes of temperature, NO, NH and NH_2 with time: (a) NS hybrid 20 Td DC discharge and (b) NS discharge only.

The fast drop of NH and NH_2 density at high DC E/N values can be explained from the view point of the classical combustion chemistry: the increased temperature (2900 K for DC E/N=20Td, see Fig. 7) leads to more H, O and OH radicals that rapidly consume NH and NH_2, while at lower temperature, these radicals are bonded in water molecules.

4. Conclusion

This work investigates the effects of hybrid NS and DC discharges on the ignition delay and NO production in the $NH_3/O_2/N_2$ mixture. A zero–dimensional plasma–combustion coupled solver with sensitivity and path flux analysis module is developed based on the ZDPlaskin package and a home–made combustion chemistry code. The plasma and combustion chemistry mechanisms are reviewed and improved. The electron impact cross sections of NH_3 are checked by data from PT experiments, the influence of vibrationally excited states, $NH_3(v)$, $N_2(v)$ and $O_2(v)$, are taken into account with estimated rates. The ignition process of $NH_3/O_2/N_2$ mixture under the influence of 200 Td NS hybrid 0–20 Td DC discharges are calculated, the following conclusions are drawn:

(i) The DC fields of 5–20 Td between pluses reduce the ignition delay time by 1–2 orders of magnitudes in $NH_3/O_2/N_2$ mixture. O and OH are not the main reasons for the reduction of ignition delay time but $O(^1D)$ shows a strong kinetic enhancement on ignition via $NH_3 + O(^1D) \rightarrow NH_2 + OH$. The vibrationally excited states $NH_3(v2)$ dominates the heat release before ignition through V–T relaxation reaction ($NH_3(v2) + NH_3 \rightarrow 2NH_3$).

(ii) $O_2(a^1\Delta_g)$ density increase significantly with E/N values in the DC stages. There are two main pathways of $O_2(a^1\Delta_g)$ consumption: $O_2(a^1\Delta_g) + H_2 \rightarrow$ product and $O_2(a^1\Delta_g) + H \rightarrow$ product, 90–99% of $O_2(a^1\Delta_g)$ reacts with H_2 and H to produce radicals such as O, H and OH. The rate constant for reaction $O_2(a^1\Delta_g) + NO \rightarrow O_2 + NO$ needs to be used correctly ($2.5 \times 10^{-17} cm^3/s$ instead of $2.5 \times 10^{-11} cm^3/s$), otherwise, 99% of the $O_2(a^1\Delta_g)$ will quenched by NO instead of reacting with H_2/H, thus underestimating the kinetic enhancement of $O_2(a^1\Delta_g)$ on ignition.

(iii) NS hybrid DC discharge will lead to an increase in NO: the NO density at hybrid 20 Td is nearly twice as that driven only by NSD. A peak density of $4 \times 10^{16} cm^{-3}$ is achieved in this work in condition of 1000 K and atmospheric pressure.

(iv) Both the production and the consumption of NO molecules is related closely with NH_3. NO originates mainly from NH (12–16%), HNO (45–58%), N (0–9%) and $N_2(v)$ (0–20%), and the majority of NO are consumed by colliding with NH and NH_2 molecules (91–94%) at low DC E/N field (0–5 Td), leading to the production of H, OH and NNH radicals. At higher DC E/N values (10–20 Td), the contribution of NH and NH_2 molecules drops to 78–83%, the influence of N and NNH becomes significant. The rapid increase of NO caused by hybrid DC discharge is unique in the NH_3/air mixture.

The basic conclusion that NO_x emission will increase in presence of low DC fields between pulses leads to the possibility of plasma assisted fixation by discharges with “Pulse–DC” like electric waveform, e.g., the NS hybrid DC discharge plasma used in this study has many similar characteristics to the gliding arc discharges: both operate at high temperature (≈1000 K), both have high and low electric field periods, both have a long period with relatively low field. But the existence of equilibrium–to–nonequilibrium transition, the heat convection with ambient flow and the constant changing field post many challenges and will be studied in future works.

Novelty and significance statement

The plasma–combustion coupled chemistry mechanism is developed for ignition delay and NO_x prediction, experimentally validated cross sections and the contribution of vibrationally excited species are taken into considerations. The production/loss of NO_x, which is one of the main concerns in ammonia/air ignition/combustion is analyzed, and the effect of long–lived $O_2(a^1\Delta_g)$ is revealed after correcting the rate constant of $O_2(a^1\Delta_g) + NO \rightarrow O_2 + NO$. The conclusions of this paper will facilitate the community of plasma assisted ignition/combustion in designing ignition devices for NH_3 containing mixtures.

Declaration of Competing Interest

The authors declare that they have no known competing financial interests or personal relationships that could have appeared to influence the work reported in this paper.

CRediT authorship contribution statement

Yifan Qiu: Writing – original draft, Formal analysis, Data curation. **Yifei Zhu:** Writing – review & editing, Conceptualization, Supervision. **Yun Wu:** Funding acquisition, Project administration. **Ningqiu Zhao:** Investigation. **Zhenyang Li:** Investigation. **Mai Hao:** Investigation. **Boya Zhang:** Validation. **Di Pan:** Software.

Acknowledgments

The work is supported by the National Natural Science Foundation of China No. 52277168 and 52025064. The authors are thankful to the young research group in Atelier des Plasmas for fruitful discussions.

Supplementary material

Supplementary material associated with this article can be found, in the online version, at doi:10.1016/j.combustflame.2023.113078.

References

[1] A. Valera-Medina, H. Xiao, M. Owen-Jones, W.I. David, P. Bowen, Ammonia for power, Prog. Energy Combust. Sci. 69 (2018) 63–102.
[2] H. Kobayashi, A. Hayakawa, K.K.A. Somarathne, E.C. Okafor, Science and technology of ammonia combustion, Proc. Combust. Inst. 37 (1) (2019) 109–133.
[3] L. Kang, W. Pan, J. Zhang, W. Wang, C. Tang, A review on ammonia blends combustion for industrial applications, Fuel 332 (2023) 126150.
[4] C. Duynslaegher, H. Jeanmart, J. Vandooren, Ammonia combustion at elevated pressure and temperature conditions, Fuel 89 (11) (2010) 3540–3545.
[5] W. Kim, M.G. Mungal, M.A. Cappelli, The role of in situ reforming in plasma enhanced ultra lean premixed methane/air flames, Combust. Flame 157 (2) (2010) 374–383.
[6] A. Starikovskiy, N. Aleksandrov, Plasma-assisted ignition and combustion, Prog. Energy Combust. Sci. 39 (1) (2013) 61–110.
[7] K. Takita, T. Uemoto, T. Sato, Y. Ju, G. Masuya, K. Ohwaki, Ignition characteristics of plasma torch for hydrogen jet in an airstream, J. Propul. Power 16 (2) (2000) 227–233.
[8] Y. Ju, J.K. Lefkowitz, C.B. Reuter, S.H. Won, X. Yang, S. Yang, W. Sun, Z. Jiang, Q. Chen, Plasma assisted low temperature combustion, Plasma Chem. Plasma Process. 36 (2016) 85–105.
[9] T. Ombrello, Y. Ju, A. Fridman, Kinetic ignition enhancement of diffusion flames by nonequilibrium magnetic gliding arc plasma, AIAA J. 46 (10) (2008) 2424–2433.
[10] G. Faingold, J.K. Lefkowitz, A numerical investigation of $NH_3/O_2/He$ ignition limits in a non-thermal plasma, Proc. Combust. Inst. 38 (4) (2021) 6661–6669.
[11] X. Zhu, Y. Zhao, M. Zhai, P. Lv, W. Zhou, B. Huang, Investigation on spectral characteristics of gliding arc plasma assisted ammonia lean combustion, Processes 10 (9) (2022) 1750.
[12] Q. Lin, Y. Jiang, C. Liu, L. Chen, W. Zhang, J. Ding, J. Li, Controllable NO emission and high flame performance of ammonia combustion assisted by non-equilibrium plasma, Fuel 319 (2022) 123818.
[13] M. Shahsavari, A.A. Konnov, A. Valera-Medina, M. Jangi, On nanosecond plasma-assisted ammonia combustion: effects of pulse and mixture properties, Combust. Flame 245 (2022) 112368.
[14] T.S. Taneja, P.N. Johnson, S. Yang, Nanosecond pulsed plasma assisted combustion of ammonia-air mixtures: effects on ignition delays and NOx emission, Combust. Flame 245 (2022) 112327.
[15] H. Zhong, N. Liu, X. Mao, Z. Wang, Y. Ju, Kinetic studies of low-temperature ammonia oxidation in a nanosecond repetitively-pulsed discharge, AIAA SCITECH 2023 Forum (2023), p. 1694.
[16] X. Mao, H. Zhong, N. Liu, Y. Ju, Ignition enhancement of NH_3/air mixtures by non-equilibrium excitation in a nanosecond pulsed plasma discharge, AIAA SCITECH 2023 Forum (2023), p. 0748.
[17] H. Zhong, X. Mao, N. Liu, Z. Wang, T. Ombrello, Y. Ju, Understanding non-equilibrium N_2O/NOx chemistry in plasma-assisted low-temperature NH_3 oxidation, Combust. Flame 256 (2023) 112948.
[18] X. Mao, Q. Chen, A.C. Rousso, T.Y. Chen, Y. Ju, Effects of controlled non-equilibrium excitation on $H_2/O_2/He$ ignition using a hybrid repetitive nanosecond and DC discharge, Combust. Flame 206 (2019) 522–535.
[19] X. Mao, A. Rousso, Q. Chen, Y. Ju, Numerical modeling of ignition enhancement of $CH_4/O_2/He$ mixtures using a hybrid repetitive nanosecond and DC discharge, Proc. Combust. Inst. 37 (4) (2019) 5545–5552.
[20] J.K. Lefkowitz, P. Guo, A. Rousso, Y. Ju, Species and temperature measurements of methane oxidation in a nanosecond repetitively pulsed discharge, Philos. Trans. R. Soc. A 373 (2048) (2015) 20140333.
[21] A.E. Lutz, R.J. Kee, J.A. Miller, SENKIN: A FORTRAN program for predicting homogeneous gas phase chemical kinetics with sensitivity analysis, Technical Report, Sandia National Labs., Livermore, CA (USA), 1988.
[22] S. Pancheshnyi, B. Eismann, G. Hagelaar, L. Pitchford, Computer code ZDPlasKin, 2008, (http://www.zdplaskin.laplace.univ-tlse.fr).
[23] A.H. Markosyan, A. Luque, F.J. Gordillo-Vázquez, U. Ebert, Pumpkin: a tool to find principal pathways in plasma chemical models, Comput. Phys. Commun. 185 (10) (2014) 2697–2702.
[24] E. Pannier, S. Ivko, QTPlaskin, 2020, (https://github.com/aluque/qtplaskin/).
[25] G. Hagelaar, L.C. Pitchford, Solving the Boltzmann equation to obtain electron transport coefficients and rate coefficients for fluid models, Plasma Sources Sci. Technol. 14 (4) (2005) 722.
[26] P.N. Brown, G.D. Byrne, A.C. Hindmarsh, VODE: a variable-coefficient ODE solver, SIAM J. Sci. Comput. 10 (5) (1989) 1038–1051.
[27] A. Flitti, S. Pancheshnyi, Gas heating in fast pulsed discharges in N_2–O_2 mixtures, Eur. Phys. J. Appl. Phys. 45 (2) (2009) 21001.
[28] A.C. Hindmarsh, ODEPACK, a systemized collection of ode solvers, Sci. Comput. (1983) 55–64.
[29] N. Popov, Fast gas heating in a nitrogen-oxygen discharge plasma: I. Kinetic mechanism, J. Phys. D: Appl. Phys. 44 (28) (2011) 285201.
[30] B. Zhang, J. Xiong, M. Hao, Y. Yao, X. Li, A.B. Murphy, Pulsed Townsend measurement of electron swarm parameters in C_4F_7N–CO_2 and C_4F_7N–N_2 mixtures as eco-friendly insulation gas, J. Appl. Phys. 131 (3) (2022).
[31] C. Powell, Electron impact ionization, Springer-Verlag: Berlin, 1985.
[32] M. Hayashi, Electron collision cross-sections determined from beam and swarm data by Boltzmann analysis, Nonequilib. Process. Partial. Ioniz. Gases 220 (1990) 333–340.
[33] Phelps database, 2022, http://www.lxcat.net, retrieved on November 1, 2022.
[34] Y. Itikawa, Cross sections for electron collisions with nitrogen molecules, J. Phys. Chem. Ref. Data 35 (1) (2006) 31–53.
[35] Y. Itikawa, Cross sections for electron collisions with oxygen molecules, J. Phys. Chem. Ref. Data 38 (1) (2009) 1–20.
[36] V. Tarnovsky, H. Deutsch, K. Becker, Cross-sections for the electron impact ionization of NDx (x=1–3), Int. J. Mass Spectrom. Ion Process. 167 (1997) 69–78.
[37] R.R. Laher, F.R. Gilmore, Updated excitation and ionization cross sections for electron impact on atomic oxygen, Phys. Chem. Ref. Data 19 (1) (1990) 277–305.
[38] R.J. Henry, P. Burke, A.-L. Sinfailam, Scattering of electrons by C, N, O, N^+, O^+, and O^{++}, Phys. Rev. 178 (1) (1969) 218.
[39] Y. Itikawa, N. Mason, Cross sections for electron collisions with water molecules, J. Phys. Chem. Ref. Data 34 (1) (2005) 1–22.
[40] S. Matejcik, A. Kiendler, P. Cicman, J. Skalny, P. Stampfli, E. Illenberger, Y. Chu, A. Stamatovic, T. Märk, Electron attachment to molecules and clusters of atmospheric relevance: oxygen and ozone, Plasma Sources Sci. Technol. 6 (2) (1997) 140.
[41] Y. Chen, X. Jiang, L. Yao, W. Jiang, H. Liu, Y. Zhang, Electron scattering cross sections from NH_3: a comprehensive study based on R-matrix method, Plasma Sci. Technol. (2023). https://iopscience.iop.org/article/10.1088/1361-6595/acca46/meta
[42] Z. Wang, X. Han, Y. He, R. Zhu, Y. Zhu, Z. Zhou, K. Cen, Experimental and kinetic study on the laminar burning velocities of NH_3 mixing with CH_3OH and C_2H_5OH in premixed flames, Combust. Flame 229 (2021) 111392.
[43] A. Fridman, Plasma chemistry, Cambridge University Press, 2008.
[44] X. Mao, H. Zhong, T. Zhang, A. Starikovskiy, Y. Ju, Modeling of the effects of non-equilibrium excitation and electrode geometry on H_2/air ignition in a nanosecond plasma discharge, Combust. Flame 240 (2022) 112046.
[45] M. Capitelli, C.M. Ferreira, B.F. Gordiets, A.I. Osipov, Plasma kinetics in atmospheric gases, vol. 31, Springer Science & Business Media, 2013.
[46] B. Mei, X. Zhang, S. Ma, M. Cui, H. Guo, Z. Cao, Y. Li, Experimental and kinetic modeling investigation on the laminar flame propagation of ammonia under oxygen enrichment and elevated pressure conditions, Combust. Flame 210 (2019) 236–246.
[47] J. Otomo, M. Koshi, T. Mitsumori, H. Iwasaki, K. Yamada, Chemical kinetic modeling of ammonia oxidation with improved reaction mechanism for ammonia/air and ammonia/hydrogen/air combustion, Int. J. Hydrogen Energy 43 (5) (2018) 3004–3014.
[48] P. Glarborg, J.A. Miller, B. Ruscic, S.J. Klippenstein, Modeling nitrogen chemistry in combustion, Prog. Energy Combust. Sci. 67 (2018) 31–68.
[49] B.F. Gordiets, C.M. Ferreira, V.L. Guerra, J.M. Loureiro, J. Nahorny, D. Pagnon, M. Touzeau, M. Vialle, Kinetic model of a low-pressure N_2–O_2 flowing glow discharge, IEEE Trans Plasma Sci 23 (4) (1995) 750–768.

[50] M. Yaron, A. Von Engel, P. Vidaud, The collisional quenching of $O_2^*(^1\Delta_g)$ by NO and CO_2, Chem. Phys. Lett 37 (1) (1976) 159–161.
[51] R.B. Boodaghians, P.M. Borrell, P. Borrell, Room-temperature rate constants for the gas-phase quenching of metastable molecular oxygen, $O_2(a^1\Delta_g)$ and $O_2(b^1\Sigma_g+)$, by CO_2, N_2O, NO,NH_3, HCl and SO_2, Chem. Phys. Lett 97 (2) (1983) 193–197.
[52] N. Popov, Evolution of the negative ion composition in the afterglow of a streamer discharge in air, Plasma Phys. Rep. 36 (2010) 812–818.
[53] J. Payzant, P. Kebarle, Kinetics of reactions leading to $O_2^-(H_2O)_n$ in moist oxygen, J. Chem. Phys. 56 (7) (1972) 3482–3487.